Title

Design Principles for Two-Dimensional Molecular Aggregates Using Kasha's Model: Tunable Photophysics in Near and Short-Wave Infrared

Journal

The Journal of Physical Chemistry C, 123(30)

ISSN

1932-7447

Authors

Deshmukh, Arundhati P
Koppel, Danielle
Chuang, Chern
et al.

Publication Date

2019-08-01

DOI

10.1021/acs.jpcc.9b05060

Peer reviewed

THE JOURNAL OF PHYSICAL CHEMISTRY C

Article

Cite This: J. Phys. Chem. C XXXX, XXX, XXX−XXX

pubs.acs.org/JPCC

Design Principles for Two-Dimensional Molecular Aggregates Using Kasha's Model: Tunable Photophysics in Near and Short-Wave Infrared

Arundhati P. Deshmukh,[†] Danielle Koppel,[†] Chern Chuang,[‡] Danielle M. Cadena,[†] Jianshu Cao,[§] and Justin R. Caram*[,†]

[†]Department of Chemistry and Biochemistry, University of California, Los Angeles, 607 Charles E. Young Dr. East, Los Angeles, California 90095, United States

[‡]Department of Chemistry, University of Toronto, 80 St. George Street, Toronto, Ontario M5S 3H6, Canada

[§]Department of Chemistry, Massachusetts Institute of Technology, Cambridge, Massachusetts 02139, United States

Supporting Information

ABSTRACT: Technologies which utilize near-infrared (NIR) (700−1000 nm) and short-wave infrared (1000−2000 nm) electromagnetic radiation have applications in deep-tissue imaging, telecommunications, and satellite telemetry due to low scattering and decreased background signal in this spectral region. It is therefore necessary to develop materials that absorb light efficiently beyond 1000 nm. Transition dipole moment coupling (e.g., J-aggregation) allows for red-shifted excitonic states and provides a pathway to highly absorptive electronic states in the infrared. We present aggregates of two cyanine dyes whose absorption peaks red-shift dramatically upon aggregation in water from ∼800 to 1000 nm and 1050 nm, respectively, with sheet-like morphologies and high molar absorptivities ($\varepsilon \approx 10^5$ M^{-1} cm^{-1}). We use Frenkel exciton theory to extend Kasha's model for J- and H-aggregations and describe the excitonic states of two-dimensional aggregates whose slip is controlled by steric hindrance in the assembled structure. A consequence of the increased dimensionality is the phenomenon of an intermediate "I-aggregate", one which red-shifts yet displays spectral signatures of band-edge dark states akin to an H-aggregate. We distinguish between H-, I-, and J-aggregates by showing the relative position of the bright (absorptive) state within the density of states using temperature-dependent spectroscopy. I-aggregates hold potential for applications such as charge injection moieties for semiconductors and donors for energy transfer in NIR and short-wave infrared. Our results can be used to better design chromophores with predictable and tunable aggregation with new photophysical properties.

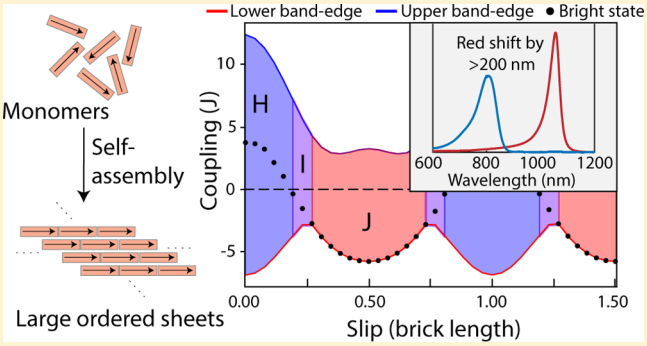

INTRODUCTION

Near-infrared (NIR, 700−1000 nm) and short-wave infrared (SWIR, 1000−2000 nm) photoactive materials are highly sought out because of their superior performance in many applications, ranging from deep-tissue imaging[1] to telecommunications[2] and LIDAR.[3] Light in the NIR and SWIR transmits over longer distances in the atmosphere and shows less loss for fiber-optic communication because of decreased scatter and absorption in this spectral regime.[2] In biomedical contexts, significantly decreased auto-fluorescence from biomolecules in the SWIR promotes better signal-to-noise ratio in fluorescence imaging.[4−6]

However, there are few molecular species (such as carbon nanotubes, lanthanide complexes, and flavylium polymethine dyes), which absorb efficiently beyond 1000 nm.[5,7] Approaches for designing strong absorbers and emitters in NIR and SWIR are primarily based on covalent modification of conjugated dyes and semiconductor nanocrystal materials.[7−10] These materials cannot necessarily offer high molar absorptivities and narrow linewidths, prerequisites for several technological applications such as nonlinear optics and photonics.[11,12] However, another approach to achieving strong SWIR absorption is through coupling of multiple molecular transition dipole moments (TDMs, μ) into extended excitonic states. The oscillator strength and radiative rate of a molecule are proportional to the square of the TDM ($\mu^2 = |\langle g|\Sigma_i q_i r_i|e\rangle|^2$, where g and e represent the ground and excited state wavefunctions, q_i and r_i are the charges and their positions).[13] In molecular aggregates, certain excitonic transitions are enhanced by a nonlinear increase in the oscillator strength due to long-range coherent coupling among TDMs.[14] Molecular aggregates, therefore, can show increased absorption

Received: May 28, 2019
Revised: July 5, 2019
Published: July 9, 2019

DOI: 10.1021/acs.jpcc.9b05060
J. Phys. Chem. C XXXX, XXX, XXX−XXX

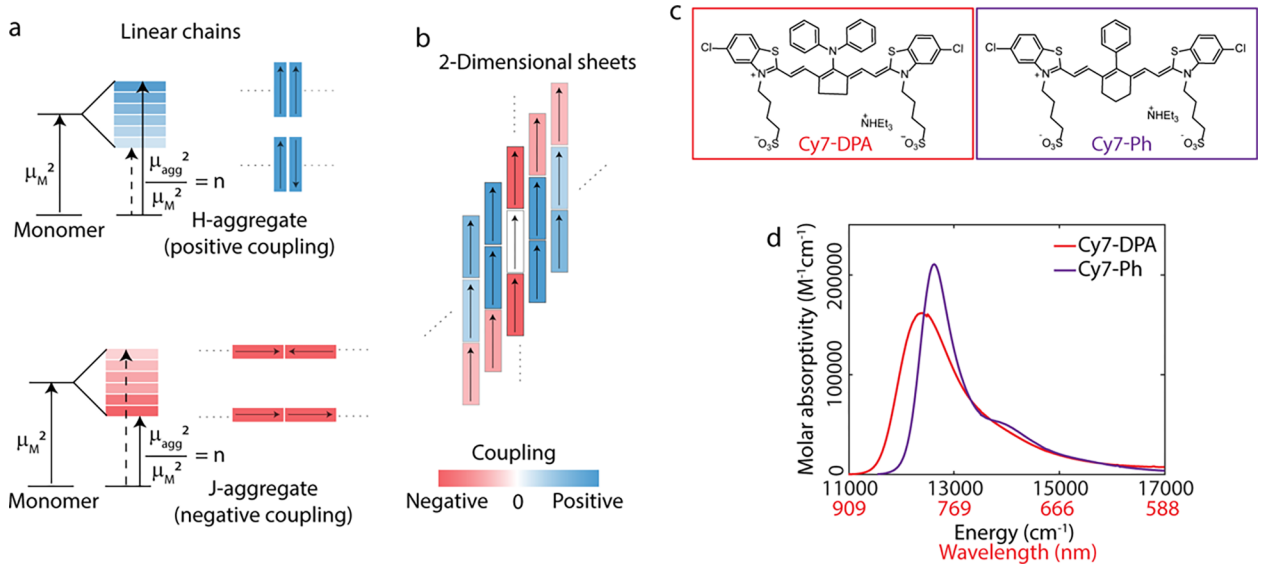

Figure 1. (a) Schematic depicting H- and J-aggregations for dimers and linear chain aggregates based on Kasha's model (ref 19), where n is the number of monomers in the chain and μ_M and μ_{agg} denote TDMs of the monomer and aggregate, respectively, (b) Schematic depiction of coupling of a central brick (white) within a 2D aggregate with its neighbors, (c) molecular structures of the cyanine dyes investigated, and (d) absorption spectra of the dyes in their monomeric form in methanol solutions.

over a narrower wavelength range, enhanced emission due to faster radiative rates, and long-range coherent energy transport.[14−17]

To begin, we define molecular aggregates as noncovalently bound molecular assemblies formed via entropic and van der Waals driving forces.[14] Molecules within an aggregate undergo coherent TDM coupling, and electronic excitations extend over many molecules to form delocalized Frenkel excitons.[18] The net excitonic TDM depends on the phase relationship of individual TDMs, their coupling, both defined by the geometric arrangement of dipoles, and the energetic disorder among the chromophores.[14] Kasha developed a simple formalism describing how aggregation leads to absorption shifts for molecular dimers and linear chain aggregates as shown in Figure 1a.[19] When dipoles are aligned in a head-to-tail fashion, the optically active bright state (with nonzero TDM) is also the lowest energy exciton. As a result, these arrangements give rise to a redshift in the absorption spectrum. On the other hand, cofacial dye organization renders the highest energy exciton as the only optically active state resulting in a blue shift in the absorption spectrum. The blue-shifted aggregates are called H-aggregates, whereas the red-shifted aggregates are called J-aggregates.[14,20] One can shift between H- and J-aggregations by changing the slip (or angle) between each dye monomer, and many groups have employed this approach to generate H- or J-aggregated structures.[15,21] While the formalism for dimers and linear chains is well-known,[14,19,22] complications arise in the case of 2-dimensional (2D) or quasi-2D sheet and tubular aggregates.[23] Along one axis, the predominant coupling will be negative (J-like), while coupling along the other axis could be positive (H-like). This is depicted as a cartoon in Figure 1b, where the coupling of the central brick (white) with its neighbors depends on the distance and the slip from the central brick. The net coupling would be determined by bricks along all directions. Even though several experimental[24,25] and theoretical[26,27] examples of 2D aggregates are known, general principles to tune absorption through control over molecular stacking during self-assembly are limited. In this manuscript, we show how controlling 2D aggregation slip-stacking can be used as an approach for further red-shifting the absorption, and that additional control is needed to create emissive aggregates.

Many H- and J-aggregates have been reported based on small-molecule chromophores like cyanines,[15] perylene bisimides,[28,29] porphyrins[30,31] as well as for more extended structures like conjugated polymers,[32] and pigment proteins.[14] Kasha's model and its variations[32,33] have been critical in describing the rich photophysics in such systems. We focus on cyanine dyes—a class of dyes which consist of a polymethine bridge connecting to two aromatic heterocycles. Cyanine dyes are particularly interesting because of their tendency to self-assemble into different topologies including dimers, single- and double-walled nanotubes, bundles, and sheets.[34−36] As a class, cyanine dyes exhibit large TDMs (as high as 10 D) and a high degree of structural and spectral tunability.[15,37] Recently, long-range exciton migration has been shown in double-walled nanotubes of cyanine dyes in the visible region.[38,39] Owing to these properties, cyanine dyes are extensively employed for biological imaging, Förster resonance energy transfer (FRET), and nonlinear optics and photoredox reactions.[3,4,40−42]

In this paper, we exploit a molecular aggregate structure and dimensionality to achieve new materials with high absorption cross sections above 1000 nm. Through control of solvation conditions, we observe the aggregation of two NIR thiacarbocyanines dyes (Figure 1c) into multiple morphologies (like sheets and dimers) with unique spectral shifts. Here, we focus on their most redshifted forms, which were found to be sheet-like structures with almost micron scale domains. These structures display strong ($\varepsilon \approx 10^5$ M^{-1} cm^{-1}) SWIR absorption, though little to no direct emission. To connect the observed photophysics to the structure, we construct an analytical model based on long-range TDM coupling and calculate the density of states (DOS) and other optical properties. Unique to the sheet morphology, we describe an "I-aggregate" one which exhibits intermediate photophysics between J- and H-aggregates, a red-shifting yet nonemissive

DOI: 10.1021/acs.jpcc.9b05060
J. Phys. Chem. C XXXX, XXX, XXX−XXX

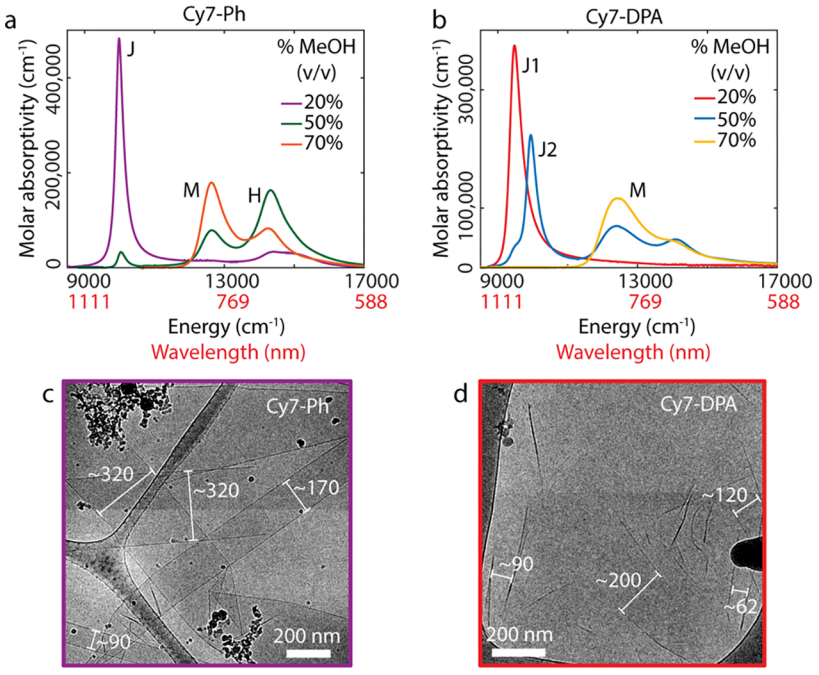

Figure 2. Top: selected absorption spectra of (a) Cy7-Ph and (b) Cy7-DPA aggregates prepared by mixing methanol solutions of the dyes with deionized water with 20, 50, and 70% methanol (v/v). Final dye concentration was kept constant (0.2 mM) for all samples. 20% samples show a sharp redshifted peak in SWIR. Bottom: cryo-electron micrographs of the most redshifted aggregates of (c) Cy7-Ph and (d) Cy7-DPA showing a 2D sheet-like morphology. Numbers indicate sheet widths in nanometers.

structure. Temperature-dependent absorption spectroscopy experimentally confirms the model, distinguishing the I- and J-aggregates. Finally, we relate our results to the dye structures and induced slip, in analogy to Kasha's rules to elucidate design principles for controlling the photophysics of 2D aggregates.

EXPERIMENTAL SECTION

Materials. Cy7-DPA and Cy7-Ph were obtained from FEW chemicals GmbH (catalog nos. S0837 and S2433). Spectroscopic grade methanol, sucrose, and D-(+)-trehalose were obtained from ThermoFisher Scientific. All materials were used as obtained, without any further purification. Deionized water (18 MΩ) was used for making all samples.

Sample Preparation. Cuvettes and sample vials were presoaked in deionized water for hydrophilization. Dyes were predissolved in methanol to make different concentrations of monomer solution. The monomer solution was then added to deionized water in a specific v/v ratio to prepare the aggregate solution. All solutions were stored in foil-covered and parafilm-sealed vials for 24 h before taking any measurements. For scanning the whole % MeOH range (10−100%) while keeping the dye concentration constant, the starting concentration of monomer solution was adjusted accordingly for each sample. For concentration dependence of the H-aggregate, % MeOH was kept constant at 70% white, and the final concentration was varied (0.05−0.5 mM). Samples for temperature dependence were prepared by the sugar-matrix stabilization method previously reported.[39] Dye aggregates were first prepared in water−methanol solutions as mentioned above and stored for 24 h to let the aggregates assemble. A saturated sugar solution was made by dissolving a 50:50 sucrose/trehalose (w/w) mixture in distilled water. To a 100 μL aggregate solution, 100 μL of the saturated sugar solution was added slowly and gently mixed. This solution was drop-cast onto a 0.2 mm quartz cuvette and kept under vacuum in dark for 24 h. Cryo-electron microscopy (CryoEM) samples were prepared on mesh 200 lacey formvar/carbon copper grids obtained from Ted Pella Inc. The grids were plasma-cleaned under a H_2/O_2 gas flow using a Solarus Gatan Plasma cleaner for hydrophilization. Vitrobot Mark IV was used for plunge-freezing the samples. About 3.5 μL of the aggregate solution was dropped onto the grid, and excess solution was removed by blotting for 3.0 s with standard blotting paper from Ted Pella and immediately dropped into liquid ethane maintained close to its freezing point using liquid nitrogen. The frozen grids were stored in liquid nitrogen.

Measurements. All spectra were taken in a 0.2 mm path length quartz cuvette obtained from Starna Cells Inc. All room temperature absorption spectra were taken on a JASCO V-770 UV/Vis/NIR spectrometer. Temperature-dependent absorption measurements were performed using a Shimadzu UV/Vis/NIR spectrometer inside a liquid nitrogen-cooled Janis ST-100 cryostat. A Lakeshore 330 Autotuning Temperature Controller was used to control the temperature. CryoEM images were recorded on a FEI TF20 electron microscope equipped with a field-emission gun at 200 kV. CryoEM grids were loaded on to a Gatan 626 cryo-transfer sample holder, then inserted into the microscope, and images were taken, all under liquid nitrogen. Images were recorded on a CCD camera with 4k × 4k resolution. Image defocus was used to enhance contrast. Dynamic light scattering (DLS) experiments were performed on a Coulter Beckman dynamic light-scattering analyzer in 1 cm path length cuvettes.

RESULTS AND DISCUSSION

We obtain dyes 3,3′-bis(4-sulfobutyl)-5,5′-dichloro-11-diphenylamino-10,12-ethylenethiatricarbocyanine, ammonium salt (Cy7-DPA) and 3,3′-bis(4-sulfobutyl)-5,5′-dichloro-11-phenyl-10,12-ethylenethiatricarbocyanine, ammonium salt (Cy7-Ph) from FEW chemicals. Previous work with similar cyanine

DOI: 10.1021/acs.jpcc.9b05060
J. Phys. Chem. C XXXX, XXX, XXX−XXX

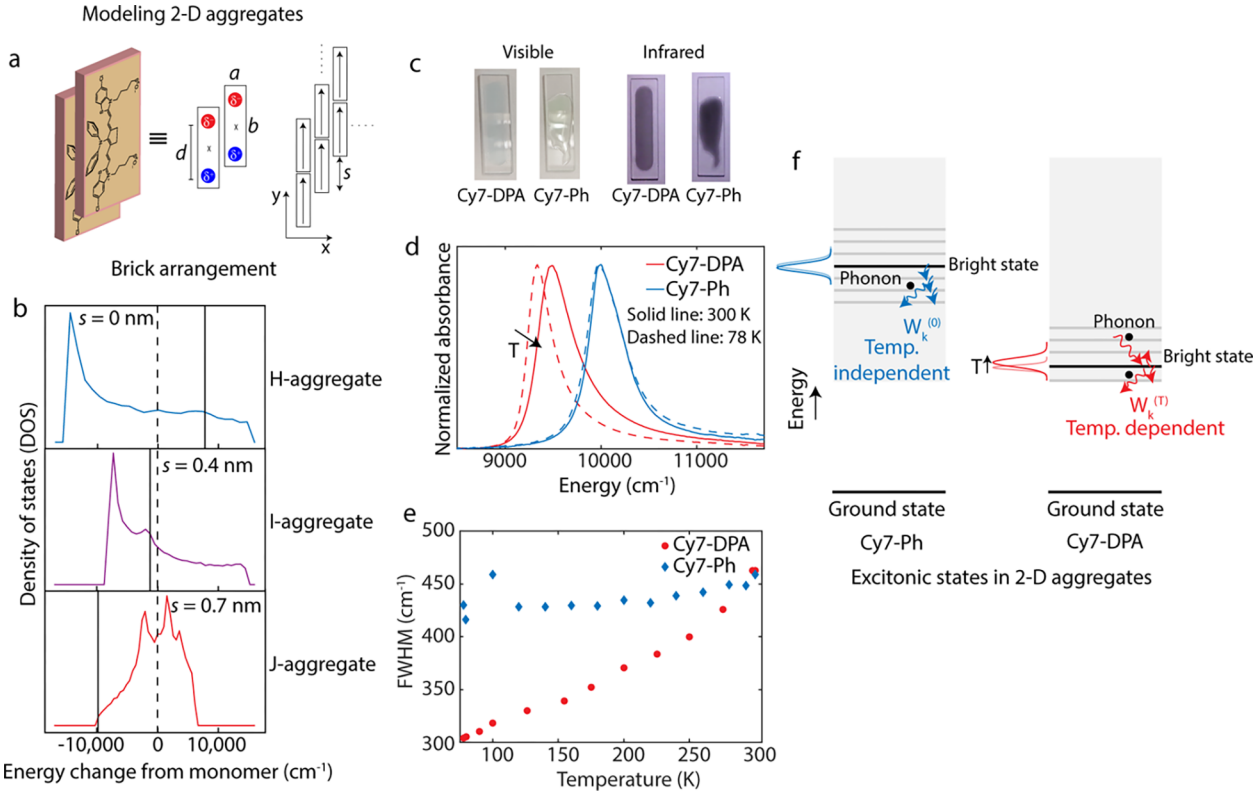

Figure 3. (a) Schematic depiction of the brick arrangement model; (b) results from the analytical model showing monomer energy (dashed line) and relative position of the bright-state (solid line) within the DOS for 0, 0.4, and 0.7 nm slips; (c) pictures of sugar matrix-stabilized aggregates as seen through a typical silicon camera with an IR filter (left) and with the IR filter removed and an 850 nm longpass filter added to remove stray light (right); (d) absorption spectra of sugar matrix-stabilized aggregates—Cy7-DPA (red) and Cy7-Ph (blue) at 300 K (solid lines) and 78 K (dashed lines); (e) fwhm of the absorption peak as a function of temperature for Cy7-DPA (red circles) and Cy7-Ph (blue diamonds); and (f) schematic describing the processes that contribute to the lineshape of Cy7-Ph and Cy7-DPA.

dyes showed sheet-like aggregation in aqueous solutions, though detailed photophysical and structural insights were not provided.[35,43,44] Cy7-DPA and Cy7-Ph dyes, shown in Figure 1c, are structurally similar to each other apart from substitutions on their cyanine bridge which do not significantly alter their monomer absorption (Figure 1d). This makes them optimal candidates for comparing the effect of the dye structure on aggregate formation and photophysics. Monomer absorption peaks of Cy7-DPA and Cy7-Ph lie in NIR at 807 nm (12 391 cm^{-1}) and 792 nm (12 626 cm^{-1}), respectively.

Adapting procedures from previous literature,[20,34] we explored the phase space of aggregation. Unlike previous aggregation routes, which use direct dissolution of dye into water or brine, pH modification, and templating,[8,35,45,46] we predissolve the dyes in methanol prior to mixing with water following the so-called "alcoholic route" to self-assembly.[47] This procedure allows for independent control over methanol−water ratios and dye concentration, and aggregates form relatively rapidly (~24 h). In Figure 2a,b, we show selected absorption spectra of aggregates where we fixed the dye concentration at 0.2 mM while varying the methanol−water ratios from 0 to 100% MeOH v/v (complete range shown in Supporting Information, Figure S1). We observe sharp red-shifted J-like aggregate peaks in SWIR at lower methanol−water ratios (% MeOH) for both the dyes. The J-like peak of Cy7-DPA lies in SWIR at ~1050 nm (9524 cm^{-1}) while that of Cy7-Ph lies at ~1000 nm (10 000 cm^{-1}). As we increase the % MeOH, the J-like peak decreases, and the monomer peak increases for both the dyes (Supporting Information Figure S1). At 50% MeOH, we observe an H-aggregate peak at 698 nm (14 327 cm^{-1}) for Cy7-Ph, whereas Cy7-DPA shows a second J-like peak (J2) at ~1000 nm (10 000 cm^{-1}) under the same conditions. We hypothesize that the diphenylamine (DPA) group in Cy7-DPA frustrates cofacial packing and as a result, we never observe an H-aggregate peak in Cy7-DPA.

We perform cryoEM on the most red-shifted samples. CryoEM of the 10% MeOH samples reveals a sheet-like morphology with large planar domains extending over hundreds of nanometers, indicating the presence of long-range order in the J-aggregates (Figure 2c,d). Similar sheet-like morphology and absorption lineshapes were observed for Cy5 and Cy7 thiacarbocyanine dye aggregates.[35,36] For a more global verification of domain sizes, we performed DLS. Estimates of domain sizes obtained from DLS agree well with cryoEM data with the smallest average across multiple trials being ~700 nm for Cy7-DPA and ~900 nm for Cy7-Ph (Supporting Information Figure S2). We were unable to isolate the J2 morphology under tested conditions. However, because of its characteristic peak shape,[35] we hypothesize that the J2 peak on Cy7-DPA also arises from a sheet morphology with slightly different dye packing. The shoulder on J2 is from some conversion to J1. From a concentration-dependent study (Supporting Information Section 2.2 and Figure S3), we assign the H-peak of Cy7-Ph to a dimer.[48]

The presence of large domains and narrow linewidths suggests that the aggregates have long-range delocalization of their TDMs. We model the aggregate photophysics following the Frenkel exciton model with extended dipole treatment

DOI: 10.1021/acs.jpcc.9b05060
J. Phys. Chem. C XXXX, XXX, XXX−XXX

developed by Kuhn and co-workers.[49,50] First, following convention,[51] we consider a monomer as a brick with an internal dipole representative of the TDM generated by single excitation (Figure 3a). We then tile the bricks with a single variable parameter, the slip (s), which represents the displacement along the long axis and construct the sheet (Figure 3a). Basing on the standard Frenkel exciton Hamiltonian[49]

$$H_s = \sum_{\mathbf{n}\neq\mathbf{m}} J(\mathbf{n},\mathbf{m})|\mathbf{n}\rangle\langle\mathbf{m}| + \sum_{n} \epsilon_{\mathbf{n}}|\mathbf{n}\rangle\langle\mathbf{n}| \quad (1)$$

where $|\mathbf{n}\rangle$ represents the state where the **n**th molecule is in the excited state while all others in the ground state, $J(\mathbf{n},\mathbf{m})$ is the excitonic coupling between the two molecules, and $\epsilon_{\mathbf{n}}$ is the individual site energy. Boundary effects are resolved by imposing periodic boundary conditions, $J(\mathbf{n},\mathbf{m}) = J(\mathbf{n}-\mathbf{m})$. We then diagonalize the Hamiltonian, $H_s = \sum_k \epsilon_k|k\rangle\langle k|$, where $|k\rangle$ is the k^{th} eigenstate with energy ϵ_k. For planar aggregates with one transition per unit cell, we obtain only a single state with finite oscillator strength $\mu_k = \mu_0|\sum_n\langle k|n\rangle|$, when all transition dipoles are in-phase (no nodes along either direction). This is the state that can absorb or emit light and is referred to as the bright state. All other excitonic states contain at least one node, and thus are optically dark. We further calculate the DOS, $D(E) = \sum_k \delta(E-\epsilon_k)$, as well as the energy of the bright state as a function of slip (see Supporting Information Section 3 and Figures S4−S7 for details) for the 2D aggregates.

The results from this model are summarized in Figure 3b, where we set $\epsilon_{\mathbf{n}} = 0$ for clarity. We observe, for 0 nm slip, an H-aggregate with the bright state blue-shifted from the monomer. For higher slip values such as 0.7 nm, we observe a typical J-aggregate with a lower band-edge bright state. Interestingly, for intermediate slip values like 0.4 nm, the bright state is still red-shifted from the monomer, but notably, not at the band-edge. We associate this case to an "I-aggregate" or intermediate aggregate as it displays a red-shifted bright state like J-aggregates but has excitonic states below the bright state, similar to H-aggregates. In other words, I-aggregates have a bright state which lies in the middle of the DOS but red-shifted from the monomer. I- and J-aggregates cannot be distinguished simply from their absorption spectra. We use their temperature-dependent linewidth to determine where the bright state sits in the DOS.

We perform temperature-dependent absorption spectroscopy on matrix-stabilized Cy7-DPA and Cy7-Ph aggregates (20% MeOH). We prepare the stabilized aggregates using a previously reported sugar matrix stabilization procedure (pictures shown in Figure 3c).[39,52] Comparison of solution and sugar matrix-stabilized aggregates (shown in Supporting Information Figure S8a) strongly suggests that the aggregate morphology remains intact in the sugar matrix. Upon cooling down from room temperature to 78 K, we find that the full-width at half maximum (FWHM) of the Cy7-DPA peak narrows from 463 to 303 cm^{-1} (34%) and red shifts by 150 cm^{-1} as shown in Figure 3d−e. On the other hand, absorption of Cy7-Ph barely changes upon cooling. The peak position of Cy7-DPA is similarly sensitive to temperature as it red-shifts upon cooling while that of Cy7-Ph barely changes (Supporting Information Figure S8b).

The effect of temperature on absorption lineshape is described by the origin of fluctuations that dephase the ground-excited state coherence. The absorption spectrum is the Fourier transform of the transition dipole autocorrelation function,[22]

$$A(t) = \langle a(t)\rangle \approx \langle e^{-i\epsilon_b t - W_b t}\rangle \quad (2)$$

where ϵ_b is the energy gap between the ground and excited state and W_b represents how system's interaction with the bath leads to energetic fluctuations that dephase the phase relationship between the ground and excited state wavefunctions. The brackets represent averaging over inhomogeneous disorder or fluctuations in the environmental degrees of freedom slower than the lifetime of the exciton. Using the Redfield framework for exciton dynamics and imposing the secular approximation and Markovian bath, we express W_b for each exciton as follows[53−55]

$$W_k = \sum_{l\neq k} \frac{O_{kl}}{e^{(\varepsilon_l-\varepsilon_k)/k_BT}-1} D_b(\varepsilon_l-\varepsilon_k) \quad (3)$$

where $O_{kl} = \sum_n |\langle k|n\rangle\langle n|l\rangle|^2$ is the wavefunction overlap between the excitonic states, k_B is the Boltzmann constant, and $D_b(E) = -D_b(-E)$ is the antisymmetrized bath spectral density. For homogeneous, translational invariant systems the secular approximation is by construct exact.[51] On the other hand, Markovian approximation is justified for the fast dissipating environment. While this is not necessarily true for the systems under consideration, as exemplified by the existence of vibronic progression observed in both monomer spectra (Figure 1d), the line width and its temperature dependence are well captured by the Markovian contribution.[49] While the inhomogeneous contribution to the linewidth is mostly temperature independent, one can further breakdown the homogeneous linewidth (or dephasing rate) W_k into (i) stimulated absorption/emission of phonons and (ii) spontaneous emission of phonons and relaxation to band-edge.

$$\begin{aligned} W_k &= \sum_{l\neq k} \frac{O_{kl}}{e^{|\varepsilon_l-\varepsilon_k|/k_BT}-1} D_b(|\varepsilon_l-\varepsilon_k|) \\ &\quad + \sum_{\varepsilon_l<\varepsilon_k} O_{kl}\cdot D_b(\varepsilon_k-\varepsilon_l) \\ &= W_k^{(T)} + W_k^{(0)} \end{aligned} \quad (4)$$

Here, $W_k^{(T)}$ represents the stimulated absorption/emission portion and thus depends on the thermal occupation of phonons (making it temperature-dependent) whereas the $W_k^{(0)}$ relies on the available DOS below the bright state and is temperature independent.[31] In Cy7-Ph aggregates, we observe minimal change with temperature, implying that the second term (relaxation to band-edge through spontaneous emission of phonons) is more dominant in the lineshape function. This implies sufficient DOS below the bright state, matching the description of an I-aggregate (Figure 3b). On the other hand, we observe a significant narrowing upon cooling in Cy7-DPA which suggests that the first term dominates the lineshape function. Therefore, Cy7-DPA must have a bright state that is thermally accessible from the band-edge. We explain this in Figure 3f where the left side shows spontaneous emission of a phonon and the subsequent relaxation to the lower energy state. This process is governed by the term $W_k^{(0)}$ of eq 4 which is temperature independent. The right side of Figure 3f shows stimulated emission of phonons, governed by $W_k^{(T)}$ which depends on the thermal occupation of phonons. As a result, the spectrum shown on the left (blue) does not change with

DOI: 10.1021/acs.jpcc.9b05060
J. Phys. Chem. C XXXX, XXX, XXX−XXX

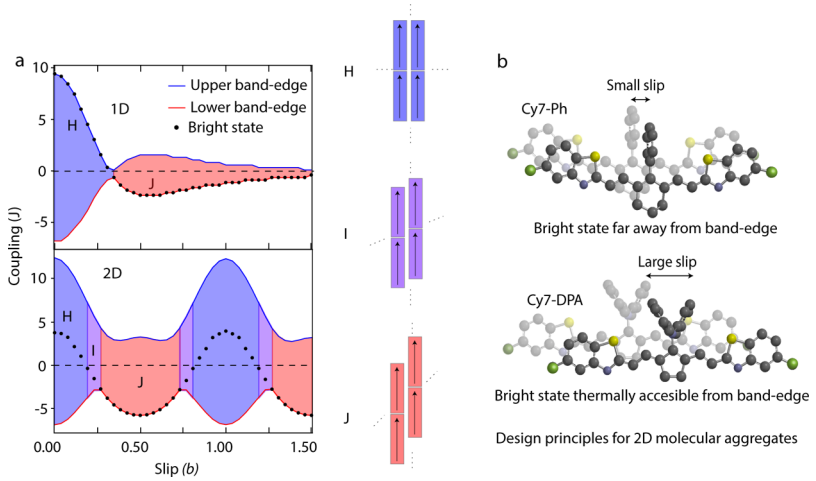

Figure 4. (a) Bright state (black dots), upper (blue), and lower (red) band edge of the excitonic band as a function of slip for 1D (top) and 2D (bottom) aggregates with non-nearest neighbor coupling. J is coupling for a head-to-tail dimer and b is the length of the brick. (b) Schematic depiction of molecular design principles for 2D aggregates (alkyl chains have been omitted for simplicity). Packing with higher slip results in a bright state closer to the band edge.

temperature while the one on right (red) broadens with increasing temperature. Simply put, when the bright state is near the band-edge, it is lineshape will be temperature-dependent. As it moves away from the band-edge, the lineshape is dominated by temperature independent relaxation within the DOS. Despite both Cy7-Ph and Cy7-DPA appearing to "J-aggregate" from their absorption spectra, the temperature dependence strongly suggests that the bright state is not at the band-edge.

Recalling Figure 3b, the differences in aggregation arise due to the slip parameter. To correlate the structural parameters (slip) and spectroscopic observables, we calculate the DOS and bright state for generalized 1D and 2D aggregates as a function of slip (Figure 4a). We use a set of general parameters shown in Table 1, which represent the average of calculations

Table 1. List of Parameters Used in the Model, a and b Are the Short and Long Axes of the Brick, Respectively, μ is the TDM, and d is the Charge Distance for the Extended Dipole (see Supporting Information for Section 3 for Details).

	a (Å)	b (Å)	μ (D)	d (Å)
Cy7-DPA	7.3	19	4.2	9
Cy7-Ph	8.8	22	4.0	3.5
generalized	8.1	21	4.1	6.3

used to determine the extended dipole parameters for Cy7-DPA and Cy7-Ph (Supporting Information Section 3.4). We express the coupling in terms of the variable J, defined as the coupling of a nearest neighbor head-to-tail dimer ($J = -2000$ cm^{-1}) calculated using the extended dipole model (eq 3 in the Supporting Information) and the slip in terms of the length of the brick (b). The maximum and minimum eigenvalues define the upper and lower band-edge of the DOS, and the region between the two extremes represents the exciton bandwidth. As seen from Figure 4a, 1D aggregates follow Kasha's framework, always displaying (upper or lower) band-edge bright states irrespective of the slip. In 2D aggregates, we observe regions H-, I-, and J-aggregations (color-coded blue, purple, and red, respectively, in Figure 4a) based on the position of the bright state within the DOS. The point where the bright state intersects the zero coupling line corresponds to a previously reported "null aggregate" meaning that there is no excitonic shift even though the exciton bandwidth is large.[56,57] Furthermore, 2D aggregates display increased possible spectral shifts due to stronger coupling. This unique band structure is a direct consequence of the 2D topology (shown in Supporting Information Figure S9) and stems novel photophysical properties of 2D aggregates.

Similar behavior plays an important role in conjugated polymer photophysics (HJ aggregates) wherein, changing the relative strength of intra-/interchain coupling gives a mid-band bright state.[57,58] While polymer networks involve covalent coupling along the polymer backbone and dipole−dipole coupling between the polymer chains, their absorption spectra have strong analogies to the van der Waals aggregates described here. It is worth mentioning that these HJ aggregates have mid-band bright states that are not necessarily red-shifted from the monomer, whereas I-aggregates have mid-band bright states red-shifted from the monomer. Furthermore, epitaxially grown 2D crystals of a perylene-based dye also resulted in a similar observation where the limited aggregate size with nonunity aspect ratios gave dark band-edge J-aggregates.[24] In this case, even with a dark band-edge, the next higher energy state was bright. Because of the extended nature of these 2D I-aggregates, the bright-state position in the DOS is a nearly continuous function of the slip as seen from Figure 4a and is thus tunable using chemical modification. Size control of self-assembled aggregates is challenging in solution. However, many SWIR applications demand solution aggregates for processability and biological compatibility. Our approach enables chemical control of the slip while also being more versatile.

Another recent theoretical investigation of 2D aggregates based on a simple dipole model demonstrates that temperature-dependent peak shifts in absorption can be related back to structural parameters like slip, however, they observe I-aggregate-like behavior at higher slips.[59] The temperature-dependent behavior of the bright state is dominated by the short-range interactions which depend strongly on the type of Hamiltonian used. Cy7-Ph shows little change in the peak position while Cy7-DPA blue-shifts with increasing temper-

DOI: 10.1021/acs.jpcc.9b05060
J. Phys. Chem. C XXXX, XXX, XXX−XXX

ature, consistent with having different slip parameters (Supporting Information Figure S8b). Using our classification scheme, we estimate that the slip for the Cy7-Ph is ∼4−5 Å and that for Cy7-DPA is between 7 and 10 Å. In general, the steric hindrance due to the DPA group will prohibit slips that are less than 7 Å (which correlates to 0.36 times its brick length), consistent with our observation that Cy7-DPA has a bright state closer to the band-edge than Cy7-Ph (Figure 4b). It is difficult to quantitatively compare our model to the experiment owing to the complexities arising from modeling the structural nature of disorder and variance in the system dielectric.[60−62] The differences induced by the substituent on the proximity of the bricks may affect the actual coupling values but they will not affect the overall behavior of H-, I-, and J-aggregations significantly.

Using an approximate slip parameter of Cy7-Ph, we introduce diagonal disorder to fit the absorption FWHM and estimate the number of sites that participate in a given exciton. Focusing on Cy7-Ph which has a narrower range of likely slip parameters, we calculate the linewidth for a range of disorder values and compare to our experimental spectra. From this, we estimate that the diagonal disorder is ∼200 cm^{-1}, and the inverse participation value is ∼8 (Supporting Information Figure S10). Despite relatively strong disorder, the high degree of coupling in a 2D aggregate enables long-range delocalization lengths even at room temperature. This strongly implies that a band picture is appropriate in describing the relevant photophysics (Supporting Information Figure S9).

CONCLUSIONS

We conclude by suggesting that in a direct analogy to 1D aggregates described by Kasha's model, 2D brick-like aggregates can be tuned through control of the slip parameter. In general, in 2D aggregates, a slip value less than 0.18 times the brick length forms an H-aggregate, while a slip value greater than 0.26 times the brick length produces a J-aggregate. Interestingly, the remaining intermediate values result in I-aggregation which shows characteristics of both J- and H-structures. The observed spectroscopic behavior of Cy7-Ph and Cy7-DPA is thus directly correlated to dye structures.

Our results demonstrate the significance of the aggregate morphology and packing as a new avenue for tuning excitonic properties. In general, 2D aggregates with strong SWIR absorption can be made by simply tuning the solvation environment of NIR dyes. However, for 2D aggregates, the position of the bright state depends on the slip and is not restricted to the band-edge unlike linear or dimer aggregate systems allowing for emergent photophysics. Using temperature dependence, we confirm that Cy7-Ph forms an I-aggregate with dark states below the bright state. Cy7-DPA also forms an I-aggregate but has a bright state closer to the band-edge because of higher slip induced by the bulkier DPA group. This may explain why both the aggregates were not emissive. Nevertheless, 2D aggregates follow a generalized classification scheme which provides a roadmap to designing custom chromophore assemblies with desired properties. For example, the central position on the cyanine bridge may be further modified with bulkier groups to induce greater slips between chromophores to achieve band-edge J-aggregates.

We can exploit the 2D topology to access unique excitonic properties and employ them for NIR and SWIR antennas. Wang and Weiss demonstrated enhanced FRET efficiency between a quantum dot pair when mediated by a SWIR absorbing J-aggregate.[40] This occurs despite the apparent low quantum yield of the aggregate, suggesting I-aggregate-mediated transport. I-aggregates present the possibility of energy transfer via dark states that can be accessed via near-field coupling similar to the LH2 complex in photosynthetic bacteria.[63] Recently, a theoretical study has shown that dark states in 2D aggregates can be accessed via near-field coupling.[64] Anantharaman et al. reported platelets of another Cy3 dye which show very small narrowing with decreasing temperature, suggesting that the platelets might be I-aggregates.[45] The interesting aspect of I-aggregates—a red-shifted bright state far away from the band-edge—provides opportunities for NIR/SWIR absorption and charge injection into another semiconductor in photovoltaics, enabling a complete utilization of the solar spectrum[32,65,66] as well as for exploring fast energy transfer from I-aggregates to enhance the emission of NIR/SWIR materials.[67] Recent studies have shown deep-tissue imaging of mice vasculature using flavylium polymethine dyes with monomeric SWIR emission.[7] Chemical modification of such dyes following the principles outlined here could enable J-aggregation, pushing them deeper into the SWIR with high molar absorptivity needed for low dosage amounts. Furthermore, these materials open the possibilities for exciton−polariton coupling at telecom relevant wavelengths for antennas and other nanoscale optical devices.[68]

ASSOCIATED CONTENT

Supporting Information

The Supporting Information is available free of charge on the ACS Publications website at DOI: 10.1021/acs.jpcc.9b05060.

Aggregation in methanol−water mixtures, DLS measurements and analysis, concentration dependence for the H-aggregate peak, details of the model construction, sugar matrix stabilization, temperature-dependent peak shifts, estimates of exciton delocalization, and band structure for 1D and 2D aggregates (PDF)

AUTHOR INFORMATION

Corresponding Author

*E-mail: jcaram@chem.ucla.edu.

ORCID

Justin R. Caram: 0000-0001-5126-3829

Author Contributions

All the authors contributed to writing the manuscript. APD did all the experiments with help from D.M.C. and D.K. performed all the computations with the help of C.C.

Notes

The authors declare no competing financial interest.

ACKNOWLEDGMENTS

We thank Prof. Ellen Sletten and Materials Characterization Laboratory at UCLA for instrumentation. We acknowledge Doran I. G. Bennet for input towards "I-aggregate" terminology. D.C. thanks Clare Booth Luce Fellowship for funding. We thank the UCLA Academic Senate for Faculty Research Grant. The authors acknowledge the use of instruments at the Electron Imaging Center for NanoMachines supported by NIH (1S10RR23057 to ZHZ) and CNSI at UCLA.

DOI: 10.1021/acs.jpcc.9b05060
J. Phys. Chem. C XXXX, XXX, XXX−XXX

REFERENCES

(1) Chen, W.; Cheng, C.; Cosco, E.; Ramakrishnan, S.; Lingg, J.; Bruns, O.; Zink, J. I.; Sletten, E. Shortwave Infrared Imaging with J-Aggregates Stabilized in Hollow Mesoporous Silica Nanoparticles. *ChemRxiv* **2018**, DOI: 10.26434/chemrxiv.7503506.v1.

(2) Hansen, M. P.; Malchow, D. S. Overview of SWIR Detectors, Cameras, and Applications. *Proc. SPIE* **2008**, *6939*, 69390I.

(3) Bouit, P.-A.; Wetzel, G.; Berginc, G.; Loiseaux, B.; Toupet, L.; Feneyrou, P.; Bretonnière, Y.; Kamada, K.; Maury, O.; Andraud, C. Near IR Nonlinear Absorbing Chromophores with Optical Limiting Properties at Telecommunication Wavelengths. *Chem. Mater.* **2007**, *19*, 5325−5335.

(4) Carr, J. A.; Franke, D.; Caram, J. R.; Perkinson, C. F.; Saif, M.; Askoxylakis, V.; Datta, M.; Fukumura, D.; Jain, R. K.; Bawendi, M. G.; et al. Shortwave Infrared Fluorescence Imaging with the Clinically Approved Near-Infrared Dye Indocyanine Green. *Proc. Natl. Acad. Sci. U.S.A.* **2018**, *115*, 4465−4470.

(5) Thimsen, E.; Sadtler, B.; Berezin, M. Y. Shortwave-Infrared (SWIR) Emitters for Biological Imaging: A Review of Challenges and Opportunities. *Nanophotonics* **2017**, *6*, 1043−1054.

(6) Hong, G.; Antaris, A. L.; Dai, H. Near-Infrared Fluorophores for Biomedical Imaging. *Nat. Biomed. Eng.* **2017**, *1*, 0010.

(7) Cosco, E. D.; Caram, J. R.; Bruns, O. T.; Franke, D.; Day, R. A.; Farr, E. P.; Bawendi, M. G.; Sletten, E. M. Flavylium Polymethine Fluorophores for Near- and Shortwave Infrared Imaging. *Angew. Chem., Int. Ed.* **2017**, *56*, 13126−13129.

(8) Wang, C.; Weiss, E. A. Sub-Nanosecond Resonance Energy Transfer in the Near-Infrared within Self-Assembled Conjugates of PbS Quantum Dots and Cyanine Dye J-Aggregates. *J. Am. Chem. Soc.* **2016**, *138*, 9557−9564.

(9) Levitz, A.; Marmarchi, F.; Henary, M. Introduction of Various Substitutions to the Methine Bridge of Heptamethine Cyanine Dyes: Via Substituted Dianil Linkers. *Photochem. Photobiol. Sci.* **2018**, *17*, 1409−1416.

(10) Bricks, J. L.; Kachkovskii, A. D.; Slominskii, Y. L.; Gerasov, A. O.; Popov, S. V. Molecular Design of near Infrared Polymethine Dyes: A Review. *Dyes Pigm.* **2015**, *121*, 238−255.

(11) Boyd, G. T. Applications Requirements for Nonlinear-Optical Devices and the Status of Organic Materials. *J. Opt. Soc. Am. B* **1989**, *6*, 685.

(12) Thomas, R.; Thomas, A.; Pullanchery, S.; Joseph, L.; Somasundaran, S. M.; Swathi, R. S.; Gray, S. K.; Thomas, K. G. Plexcitons: The Role of Oscillator Strengths and Spectral Widths in Determining Strong Coupling. *ACS Nano* **2017**, *12*, 402−415.

(13) Hilborn, R. C. Einstein Coefficients, Cross Sections, f Values, Dipole Moments, and All That. *Am. J. Physiol.* **1982**, *50*, 982.

(14) Brixner, T.; Hildner, R.; Köhler, J.; Lambert, C.; Würthner, F. Exciton Transport in Molecular Aggregates - From Natural Antennas to Synthetic Chromophore Systems. *Adv. Energy Mater.* **2017**, *7*, 1700236.

(15) Bricks, J. L.; Slominskii, Y. L.; Panas, I. D.; Demchenko, A. P. Fluorescent J-Aggregates of Cyanine Dyes: Basic Research and Applications Review. *Methods Appl. Fluoresc.* **2017**, *6*, 012001.

(16) Doria, S.; Sinclair, T. S.; Klein, N. D.; Bennett, D. I. G.; Chuang, C.; Freyria, F. S.; Steiner, C. P.; Foggi, P.; Nelson, K. A.; Cao, J.; et al. Photochemical Control of Exciton Superradiance in Light-Harvesting Nanotubes. *ACS Nano* **2018**, *12*, 4556−4564.

(17) Zhu, T.; Wan, Y. Direct Imaging of Frenkel Exciton Transport by Ultrafast Microscopy. *Acc. Chem. Res.* **2017**, *50*, 1725−1733.

(18) Scholes, G. D.; Rumbles, G. Erratum: Excitons in nanoscale systems. *Nat. Mater.* **2006**, *5*, 920.

(19) Kasha, M. Energy Transfer Mechanisms and the Molecular Exciton Model for Molecular Aggregates. *Radiat. Res.* **1963**, *20*, 55−71.

(20) Jelley, E. E. Spectral Absorption and Fluorescence of Dyes in the Molecular State. *Nature* **1936**, *138*, 1009−1010.

(21) Kaiser, T. E.; Stepanenko, V.; Würthner, F. Fluorescent J-Aggregates of Core-Substituted Perylene Bisimides: Studies on Structure−Property Relationship, Nucleation−Elongation Mechanism, and Sergeants-and-Soldiers Principle. *J. Am. Chem. Soc.* **2009**, *131*, 6719−6732.

(22) May, V.; Kühn, O. *Charge and Energy Transfer Dynamics in Molecular Systems*, 3rd ed.; Wiley-VCH: Berlin, 2011.

(23) Nabetani, A.; Tomioka, A.; Tamaru, H.; Miyano, K. Optical Properties of Two-dimensional Dye Aggregate. *J. Chem. Phys.* **1995**, *102*, 5109−5117.

(24) Eisfeld, A.; Marquardt, C.; Paulheim, A.; Sokolowski, M. Superradiance from Two Dimensional Brick-Wall Aggregates of Dye Molecules: The Role of Size and Shape for the Temperature Dependence. *Phys. Rev. Lett.* **2017**, *119*, 097402.

(25) Prokhorov, V. V.; Perelygina, O. M.; Pozin, S. I.; Mal'tsev, E. I.; Vannikov, A. V. Polymorphism of Two-Dimensional Cyanine Dye J-Aggregates and Its Genesis: Fluorescence Microscopy and Atomic Force Microscopy Study. *J. Phys. Chem. B* **2015**, *119*, 15046−15053.

(26) Möbius, D.; Kuhn, H. Energy Transfer in Monolayers with Cyanine Dye Sheibe Aggregates. *J. Appl. Phys.* **1988**, *64*, 5138−5141.

(27) Bakalis, L. D.; Rubtsov, I.; Knoester, J. Absorption Spectra of Mixed Two-Dimensional Cyanine Aggregates on Silver Halide Substrates. *J. Chem. Phys.* **2002**, *117*, 5393−5403.

(28) Wolter, S.; Magnus Westphal, K.; Hempel, M.; Würthner, F.; Kühn, O.; Lochbrunner, S. Low Temperature Exciton Dynamics and Structural Changes in Perylene Bisimide Aggregates. *J. Phys. B: At., Mol. Opt. Phys.* **2017**, *50*, 184005.

(29) Kaufmann, C.; Kim, W.; Nowak-Król, A.; Hong, Y.; Kim, D.; Würthner, F. Ultrafast Exciton Delocalization, Localization, and Excimer Formation Dynamics in a Highly Defined Perylene Bisimide Quadruple π-Stack. *J. Am. Chem. Soc.* **2018**, *140*, 4253.

(30) Wan, Y.; Stradomska, A.; Knoester, J.; Huang, L. Direct Imaging of Exciton Transport in Tubular Porphyrin Aggregates by Ultrafast Microscopy. *J. Am. Chem. Soc.* **2017**, *139*, 7287−7293.

(31) Wan, Y.; Stradomska, A.; Fong, S.; Guo, Z.; Schaller, R. D.; Wiederrecht, G. P.; Knoester, J.; Huang, L. Exciton Level Structure and Dynamics in Tubular Porphyrin Aggregates. *J. Phys. Chem. C* **2014**, *118*, 24854−24865.

(32) Hestand, N. J.; Spano, F. C. Molecular Aggregate Photophysics beyond the Kasha Model: Novel Design Principles for Organic Materials. *Acc. Chem. Res.* **2017**, *50*, 341−350.

(33) Zheng, C.; Zhong, C.; Collison, C. J.; Spano, F. C. Non-Kasha Behavior in Quadrupolar Dye Aggregates: The Red-Shifted H-Aggregate. *J. Phys. Chem. C* **2019**, *123*, 3203−3215.

(34) Eisele, D. M.; Arias, D. H.; Fu, X.; Bloemsma, E. A.; Steiner, C. P.; Jensen, R. A.; Rebentrost, P.; Eisele, H.; Tokmakoff, A.; Lloyd, S.; et al. Robust Excitons Inhabit Soft Supramolecular Nanotubes. *Proc. Natl. Acad. Sci. U.S.A.* **2014**, *111*, E3367−E3375.

(35) Berlepsch, H. V.; Böttcher, C. Tubular J-Aggregates of a New Thiacarbocyanine Cy5 Dye for the Far-Red Spectral Region-a Spectroscopic and Cryo-Transmission Electron Microscopy Study. *Phys. Chem. Chem. Phys.* **2018**, *20*, 18969−18977.

(36) Berlepsch, H. V.; Böttcher, C. Cryo-Transmission Electron Microscopy Reveals Mesoscopic H- and J-Aggregates of near Infrared Cyanine Dyes. *J. Photochem. Photobiol., A* **2010**, *214*, 16−21.

(37) Vitukhnovsky, A. G.; Lobanov, A. N.; Pimenov, A.; Yonezawa, Y.; Kometani, N.; Asami, K.; Yano, J. Absorption Spectra Simulation of Amalgamation-Type Cyanine Dye Aggregates in LB Films. *J. Lumin.* **2000**, *87*−*89*, 260−262.

(38) Clark, K. A.; Krueger, E. L.; Vanden Bout, D. A. Direct Measurement of Energy Migration in Supramolecular Carbocyanine Dye Nanotubes. *J. Phys. Chem. Lett.* **2014**, *5*, 2274−2282.

(39) Caram, J. R.; Doria, S.; Eisele, D. M.; Freyria, F. S.; Sinclair, T. S.; Rebentrost, P.; Lloyd, S.; Bawendi, M. G. Room-Temperature Micron-Scale Exciton Migration in a Stabilized Emissive Molecular Aggregate. *Nano Lett.* **2016**, *16*, 6808−6815.

(40) Wang, C.; Weiss, E. A. Accelerating FRET between Near-Infrared Emitting Quantum Dots Using a Molecular J-Aggregate as an Exciton Bridge. *Nano Lett.* **2017**, *17*, 5666−5671.

(41) Eisele, D. M.; Berlepsch, H. V.; Böttcher, C.; Stevenson, K. J.; Vanden Bout, D. A.; Kirstein, S.; Rabe, J. P. Photoinitiated Growth of

DOI: 10.1021/acs.jpcc.9b05060
J. Phys. Chem. C XXXX, XXX, XXX−XXX

Sub-7 Nm Silver Nanowires within a Chemically Active Organic Nanotubular Template. *J. Am. Chem. Soc.* **2010**, *132*, 2104−2105.
(42) Freyria, F. S.; Cordero, J. M.; Caram, J. R.; Doria, S.; Dodin, A.; Chen, Y.; Willard, A. P.; Bawendi, M. G. Near-Infrared Quantum Dot Emission Enhanced by Stabilized Self-Assembled J-Aggregate Antennas. *Nano Lett.* **2017**, *17*, 7665−7674.
(43) Scheblykin, I. G.; Sliusarenko, O. Y.; Lepnev, L. S.; Vitukhnovsky, A. G.; Van der Auweraer, M. Excitons in Molecular Aggregates of 3,3′-Bis-[3-Sulfopropyl]-5,5′-Dichloro-9- Ethylthiacarbocyanine (THIATS): Temperature Dependent Properties. *J. Phys. Chem. B* **2001**, *105*, 4636−4646.
(44) Scheblykin, I. G.; Bataiev, M. M.; Van der Auweraer, M.; Vitukhnovsky, A. G. Dimensionality and Temperature Dependence of the Radiative Lifetime of J-Aggregates with Davydov Splitting of the Exciton Band. *Chem. Phys. Lett.* **2000**, *316*, 37−44.
(45) Anantharaman, S. B.; Stöferle, T.; Nüesch, F. A.; Mahrt, R. F.; Heier, J. Exciton Dynamics and Effects of Structural Order in Morphology-Controlled J-Aggregate Assemblies. *Advanced Functional Materials*; John Wiley & Sons, Ltd., Dec 20, 2018; p 1806997.
(46) Misawa, K.; Ono, H.; Minoshima, K.; Kobayashi, T. New Fabrication Method for Highly Oriented J Aggregates Dispersed in Polymer Films. *Appl. Phys. Lett.* **1993**, *63*, 577−579.
(47) Eisele, D. M.; Cone, C. W.; Bloemsma, E. A.; Vlaming, S. M.; van der Kwaak, C. G. F.; Silbey, R. J.; Bawendi, M. G.; Knoester, J.; Rabe, J. P.; Vanden Bout, D. A. Utilizing Redox-Chemistry to Elucidate the Nature of Exciton Transitions in Supramolecular Dye Nanotubes. *Nat. Chem.* **2012**, *4*, 655−662.
(48) Takahashi, D.; Oda, H.; Izumi, T.; Hirohashi, R. Substituent Effects on Aggregation Phenomena in Aqueous Solution of Thiacarbocyanine Dyes. *Dyes Pigm.* **2005**, *66*, 1−6.
(49) Didraga, C.; Pugžlys, A.; Hania, P. R.; Von Berlepsch, H.; Duppen, K.; Knoester, J. Structure, Spectroscopy, and Microscopic Model of Tubular Carbocyanine Dye Aggregates. *J. Phys. Chem. B* **2004**, *108*, 14976−14985.
(50) Czikklely, V.; Forsterling, H. D.; Kuhn, H. Extended Dipole Model for Aggregates of Dye Molecules. *Chem. Phys. Lett.* **1970**, *6*, 207−210.
(51) Czikkely, V.; Försterling, H. D.; Kuhn, H. Light Absorption and Structure of Aggregates of Dye Molecules. *Chem. Phys. Lett.* **1970**, *6*, 11−14.
(52) Pandya, R.; Chen, R. Y. S.; Cheminal, A.; Thomas, T.; Thampi, A.; Tanoh, A.; Richter, J.; Shivanna, R.; Deschler, F.; Schnedermann, C.; et al. Observation of Vibronic-Coupling-Mediated Energy Transfer in Light-Harvesting Nanotubes Stabilized in a Solid-State Matrix. *J. Phys. Chem. Lett.* **2018**, *9*, 5604−5611.
(53) Mukamel, S. *Principles of Nonlinear Optical Spectroscopy*; Oxford University Press: New York, 1995.
(54) Heijs, D. J.; Malyshev, V. A.; Knoester, J. Thermal Broadening of the J-Band in Disordered Linear Molecular Aggregates: A Theoretical Study. *J. Chem. Phys.* **2005**, *123*, 144507.
(55) Ma, J.; Cao, J. Förster Resonance Energy Transfer, Absorption and Emission Spectra in Multichromophoric Systems. I. Full Cumulant Expansions and System-Bath Entanglement. *J. Chem. Phys.* **2015**, *142*, 094106.
(56) Spano, F. C. Analysis of the UV/Vis and CD Spectral Line Shapes of Carotenoid Assemblies: Spectral Signatures of Chiral H-Aggregates. *J. Am. Chem. Soc.* **2009**, *131*, 4267−4278.
(57) Hestand, N. J.; Spano, F. C. Expanded Theory of H- and J-Molecular Aggregates: The Effects of Vibronic Coupling and Intermolecular Charge Transfer. *Chem. Rev.* **2018**, *118*, 7069−7163.
(58) Yamagata, H.; Spano, F. C. Interplay between Intrachain and Interchain Interactions in Semiconducting Polymer Assemblies: The HJ-Aggregate Model. *J. Chem. Phys.* **2012**, *136*, 184901.
(59) Chuang, C.; Bennett, D. I. G.; Caram, J. R.; Aspuru-Guzik, A.; Bawendi, M. G.; Cao, J. Generalized Kasha's Scheme for Classifying Two-Dimensional Excitonic Molecular Aggregates: Temperature Dependent Absorption Peak Frequency Shift. Arxiv, **2019**, arXiv:1901.01318v1.
(60) Kaiser, T. E.; Scheblykin, I. G.; Thomsson, D.; Würthner, F. Temperature-Dependent Exciton Dynamics in J-AggregatessWhen Disorder Plays a Role. *J. Phys. Chem. B* **2009**, *113*, 15836−15842.
(61) Scholes, G. D.; Fleming, G. R.; Olaya-Castro, A.; van Grondelle, R. Lessons from Nature about Solar Light Harvesting. *Nat. Chem.* **2011**, *3*, 763−774.
(62) Nugraha, A. R. T.; Saito, R.; Sato, K.; Araujo, P. T.; Jorio, A.; Dresselhaus, M. S. Dielectric Constant Model for Environmental Effects on the Exciton Energies of Single Wall Carbon Nanotubes. *Appl. Phys. Lett.* **2010**, *97*, 091905.
(63) Ferretti, M.; Hendrikx, R.; Romero, E.; Southall, J.; Cogdell, R. J.; Novoderezhkin, V. I.; Scholes, G. D.; Van Grondelle, R. Dark States in the Light-Harvesting Complex 2 Revealed by Two-Dimensional Electronic Spectroscopy. *Sci. Rep.* **2016**, *6*, 20834.
(64) Gao, X.; Eisfeld, A. Near-Field Spectroscopy of Nanoscale Molecular Aggregates. *J. Phys. Chem. Lett.* **2018**, *9*, 6003−6010.
(65) Nasr, C.; Liu, D.; Hotchandani, S.; Kamat, P. V. Dye-Capped Semiconductor Nanoclusters. Excited State and Photosensitization Aspects of Rhodamine 6G H-Aggregates Bound to SiO2 and SnO2 Colloids. *J. Phys. Chem.* **1996**, *100*, 11054−11061.
(66) Barazzouk, S.; Lee, H.; Hotchandani, S.; Kamat, P. V. Photosensitization Aspects of Pinacyanol H-Aggregates. Charge Injection from Singlet and Triplet Excited States into SnO 2 Nanocrystallites. *J. Phys. Chem. B* **2000**, *104*, 3616−3623.
(67) Lambert, C.; Koch, F.; Völker, S. F.; Schmiedel, A.; Holzapfel, M.; Humeniuk, A.; Röhr, M. I. S.; Mitric, R.; Brixner, T. Energy Transfer Between Squaraine Polymer Sections: From *Helix* to *Zigzag* and All the Way Back. *J. Am. Chem. Soc.* **2015**, *137*, 7851−7861.
(68) Saikin, S. K.; Eisfeld, A.; Valleau, S.; Aspuru-Guzik, A. Photonics Meets Excitonics: Natural and Artificial Molecular Aggregates. *Nanophotonics* **2013**, *2*, 21−38.

DOI: 10.1021/acs.jpcc.9b05060
J. Phys. Chem. C XXXX, XXX, XXX−XXX